Flexibility of the Cytoplasmic Domain of the Anion Exchange Protein, Band 3, in Human Erythrocytes

Scott M. Blackman, Eric J. Hustedt, Charles E. Cobb, and Albert H. Beth*
Department of Molecular Physiology and Biophysics, Vanderbilt University School of Medicine, Nashville, Tennessee 37232 USA

ABSTRACT The rotational flexibility of the cytoplasmic domain of band 3, in the region that is proximal to the inner membrane surface, has been investigated using a combination of time-resolved optical anisotropy (TOA) and saturation-transfer electron paramagnetic resonance (ST-EPR) spectroscopies. TOA studies of rotational diffusion of the transmembrane domain of band 3 show a dramatic decrease in residual anisotropy following cleavage of the link with the cytoplasmic domain by trypsin (E. A. Nigg and R. J. Cherry, 1980, *Proc. Natl. Acad. Sci. U.S.A.* 77:4702–4706). This result is compatible with two independent hypotheses: 1) trypsin cleavage leads to dissociation of large clusters of band 3 that are immobile on the millisecond time scale, or 2) trypsin cleavage leads to release of a constraint to uniaxial rotational diffusion of the transmembrane domain. ST-EPR studies at X- and Q-band microwave frequencies detect rotational diffusion of the transmembrane domain of band 3 about the membrane normal axis of reasonably large amplitude that does not change upon cleavage with trypsin. These ST-EPR results are not consistent with dissociation of clusters of band 3 as a result of cleavage with trypsin. Global analyses of the ST-EPR data using a newly developed algorithm indicate that any constraint to rotational diffusion of the transmembrane domain of band 3 via interactions of the cytoplasmic domain with the membrane skeleton must be sufficiently weak to allow rotational excursions in excess of 32° full-width for a square-well potential. In support of this result, analyses of the TOA data in terms of restricted amplitude uniaxial rotational diffusion models suggest that the membrane-spanning domain of that population of band 3 that is linked to the membrane skeleton is constrained to diffuse in a square-well of ~73° full-width. This degree of flexibility may be necessary for providing the unique mechanical properties of the erythrocyte membrane.

INTRODUCTION

The anion-exchange protein in human erythrocytes, also known as band 3 or AE1, is an abundant intrinsic membrane protein that is composed of two distinct domains (Steck et al., 1976; Tanner et al., 1988; Lux et al., 1989). The C-terminal transmembrane domain facilitates the exchange of bicarbonate and chloride across the membrane (see Lepke and Passow, 1976; Knauf, 1979) whereas the N-terminal cytoplasmic domain provides a site of interaction with the membrane skeleton via the bridging protein ankyrin (reviewed in Low, 1986). The interaction of the cytoplasmic domain of a subpopulation of band 3 oligomers with the membrane skeleton is critical for maintaining normal erythrocyte shape and mechanical properties (Lux and Palek, 1995; Peters et al., 1996; Southgate et al., 1996). Moreover, it has been hypothesized that the segment of the cytoplasmic domain that is proximal to the membrane surface must be flexible for the erythrocyte to exhibit normal shape and viscoelastic properties (Moriyama et al., 1992; Schofield et al., 1992; Wang, 1994). In support of this hypothesis it has been shown that a congenital defect, the deletion of nine amino acids immediately N-terminal to the first putative membrane-spanning segment, results in ovalocytic erythrocytes whose membranes are more rigid than normal, a condition known clinically as Southeast Asian ovalocytosis (Jarolim et al., 1990; reviewed in Tanner, 1997). Several experimental observations suggest that decreased flexibility of band 3 in the region joining the membrane spanning and cytoplasmic domains contributes to this phenotype (reviewed in Wang, 1994).

There exists an extensive literature on qualitative descriptions of the nature and extent of interactions between the cytoplasmic domain of band 3 and the membrane skeleton, particularly via the bridging protein ankyrin (reviewed in Low, 1986; Thevenin and Low, 1990; Michaely and Bennett, 1995; Yi et al., 1997). However, very little quantitative information has been reported with regards to the flexibility of the segment of the cytoplasmic domain between the ankyrin-binding site and the transmembrane domain. Early seminal work by Nigg and Cherry (1980) demonstrated that studies of the rotational diffusion of the transmembrane domain could provide insight into interactions of the cytoplasmic domain with the membrane skeleton. Following cleavage with trypsin at lysine 360, a procedure that severs the link between the transmembrane and cytoplasmic domains, transient dichroism studies on eosin-5-maleimide (EMA)-labeled band 3 indicated an apparent shift from immobilized species to more mobile species with a significant decrease in the residual anisotropy. The major features of these optical data, which have been duplicated in a number of subsequent studies (e.g., Matayoshi and Jovin, 1991; McPherson et al., 1993; Blackman et al., 1996), are consistent either with breaking up of large clusters of band

Received for publication 29 May 2001 and in final form 7 September 2001.
Address reprint requests to Dr. Albert H. Beth, Department of Molecular Physiology and Biophysics, Vanderbilt University School of Medicine, Nashville, TN 37232-0615. Tel.: 615-322-4235; Fax: 615-322-7236; E-mail: Al.Beth@mcmail.vanderbilt.edu.

0006-3495/01/12/3363/14 $2.00

3 that were immobile on the millisecond time scale or with the release of a constraint to uniaxial rotational diffusion (URD) experienced by that subpopulation that is linked to the membrane skeleton via the bridging protein ankyrin.

Subsequently, Hustedt and Beth (1995) showed that saturation transfer EPR (ST-EPR) spectroscopy, using a novel spin-labeled stilbene disulfonate as the molecular probe (Scothorn et al., 1996), detected URD of band 3 about the membrane normal axis of reasonably large amplitude, with a correlation time that was consistent with small oligomers (e.g., dimers or tetramers). Failure to detect a significant fraction (e.g., >10%) of highly clustered band 3 in the ST-EPR studies suggested that release of a partial constraint to rotational diffusion following cleavage with trypsin is likely to be the correct molecular interpretation of the major features of the time-resolved optical anisotropy (TOA) decays. More recently, Blackman et al. (1998a) used fluorescence resonance energy homotransfer between EMA-labeled subunits of band 3 to demonstrate that cleavage with trypsin does not significantly change the distribution of oligomeric species in ghost membranes. Moreover, the amount of homotransfer could be accounted for by small band 3 oligomers without including large contributions from a substantial fraction of highly clustered band 3. Collectively, these studies have suggested that the decrease in the residual anisotropy observed in TOA studies following cleavage with trypsin is largely the result of releasing a constraint on rotational diffusion of the transmembrane domain in the subpopulation of band 3 oligomers that are linked to the membrane skeleton. Given this working molecular level interpretation, it is possible to pose the question: what degree of flexibility does the intact linkage exhibit?

Rigorous models for the effects of constrained URD on TOA decays have been developed (e.g., Wahl, 1975; Szabo, 1984). The important general predictions from these models are that the apparent amplitudes of individual decay components and the residual anisotropy depend strongly on the magnitude of the motional constraint, but the decay times depend only weakly on the magnitude of the constraint. Rigorous models for the effects of correlation time on ST-EPR spectra for unconstrained URD (Hustedt and Beth, 1995) and for constrained URD (Hustedt and Beth, 2001) have been developed. The major effect that is exhibited in the ST-EPR spectrum is an apparent slowing of rotational diffusion as the constraint to URD is increased.

The current studies focus upon quantitating the rotational flexibility of the segment of the cytoplasmic domain of band 3 between the ankyrin-binding site and the transmembrane domain. To accomplish this goal, experimental data from labeled band 3 have been obtained and analyzed in terms of an internally consistent model using both TOA and ST-EPR. The computational algorithm described in Hustedt and Beth (2001) has been employed to define the spectral sensitivity of ST-EPR at X- and Q-band microwave frequencies to the amplitude of URD using the spin-label orientation that has been previously determined for spin-labeled band 3 (Hustedt and Beth, 1996). Calculations indicate that spectral sensitivity is greatly diminished even for a single homogeneous population of band 3 as the amplitude of URD exceeds ~60° at both microwave frequencies. The current studies demonstrate that the ST-EPR spectra obtained before and after cleavage of the cytoplasmic domain with trypsin are virtually indistinguishable. Therefore, any constraint to rotational diffusion of the transmembrane domain of that subpopulation of band 3 that interacts with the membrane skeleton must be weak enough to allow excursions that exceed this sensitivity limit of ST-EPR. Complementary time-resolved delayed fluorescence anisotropy studies indicate a significant decrease in r_∞ following cleavage with trypsin. Using an experimentally determined value for the fraction of band 3 oligomers interacting with the membrane skeleton, the change in r_∞ is consistent with an angular excursion with a full width of 73°, a value that is outside the range of high sensitivity of the V_2' ST-EPR signal at X- and Q-band microwave frequencies as demonstrated in this work. Collectively, these studies provide quantitative insights into the flexibility of the cytoplasmic domain of band 3, and they underscore the utility of complementary spectroscopic techniques for understanding the dynamics of complex protein-protein interactions. Portions of this work have been published in meeting abstracts (Blackman et al., 1998b, 1999; Hustedt et al., 2000).

MATERIALS AND METHODS

General methods

Intact erythrocytes were obtained from venous blood freshly drawn into heparinized Vacutainer tubes from normal volunteers and immediately placed on ice as described in previous work (Scothorn et al., 1996). Briefly, whole blood was diluted with 5 vol of ice-cold 113 mM sodium citrate buffer, pH 7.4 (113Cit7.4), and the erythrocytes were pelleted by centrifugation. The supernatant and buffy coat were removed by aspiration, and the cells were washed three times using 10 vol of 113Cit7.4 by repeated centrifugation, aspiration, and resuspension cycles. All preparative steps were carried out at 0–4°C unless otherwise noted.

Labeling with exogenous probes

Band 3 was spin labeled by incubating packed intact erythrocytes in 113Cit7.4 with 30 μM [^{15}N,$^{2}H_{13}$]-SL-H_2-DADS-maleimide at room temperature for 45 min (see Fig. 1) (Scothorn et al., 1996). Ten volumes of 113Cit7.4 buffer containing 0.5% bovine serum albumin (BSA; Sigma fraction V, St. Louis, MO) was added to the cells, and the sample was incubated on ice for 10 min. Following pelleting of cells by centrifugation, the cells were washed once with 10 vol of 113Cit7.4 containing 0.5% BSA (w/v) and then twice with 113Cit7.4. Band 3 was labeled with EMA (see Fig. 1; Molecular Probes, Eugene, OR) by addition of 1 vol of a 0.5 mg/ml solution of EMA (freshly prepared in 113Cit7.4) to 5 vol of erythrocytes at 50% hematocrit in 113Cit7.4 followed by incubation in the dark at room temperature for 45 min (Cobb and Beth, 1990). Unreacted EMA was removed by washing the cells with 4 vol of 113Cit7.4 containing 0.2% BSA (w/v) and followed by three washes with 113Cit7.4 alone.

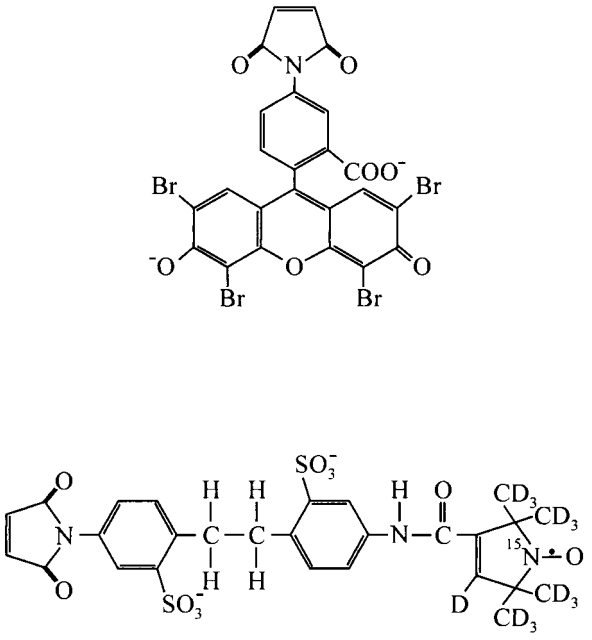

FIGURE 1 Chemical structures of eosin-5-maleimide (*top*) and [^{15}N,$^{2}H_{13}$]-SL-H_2-DADS-maleimide (*bottom*).

Preparation of ghost membranes and trypsin treatment

Ghost membranes were prepared by dropwise addition of labeled erythrocytes to 20 vol of ice-cold 5 mM sodium phosphate buffer, pH 7.4 (5P7.4) with stirring, followed by repeated centrifugation and resuspension cycles. Four or five wash cycles yielded a fluffy pellet of white (or pink, for EMA-labeled) ghost membranes. The cytoplasmic domain of band 3 was cleaved from the transmembrane domain by mild trypsin treatment essentially as described by Nigg and Cherry (1980). Briefly, ghost membranes in 5P7.4 were treated with 2 μg/ml trypsin (12,600 U/mg; Sigma) for 30 min on ice. The treated ghost membranes were washed once with 5P7.4 containing 30 μg/ml phenylmethylsulfonyl fluoride (Sigma) and then three times with 5P7.4. Cleavage of the cytoplasmic domain of band 3 was $\geq$90% with minimal cleavage of other major erythrocyte membrane proteins as assessed by SDS-polyacrylamide gel electrophoresis (SDS-PAGE) (Laemmli, 1970). All preparative procedures on EMA-labeled cells were carried out in the dark to avoid photo-induced cross-linking of band 3.

Determination of the fraction of membrane-skeleton-attached band 3

EMA-labeled band 3 was extracted from control or trypsin-treated ghost membranes by incubating 1 vol of packed ghosts with 20 vol of 5P7.4 containing 0.5, 1.0, or 2.0% $C_{12}E_8$ (w/v; Nikko Chemical Co., Tokyo, Japan) on ice for 1, 10, or 60 min. The samples were centrifuged at 15,000 $\times$ *g* for 20 min at 4°C, and an aliquot of the supernatant was carefully removed, to which 20% sodium dodecyl sulfate (SDS; w/v; Fisher Scientific, Fair Lawn, NJ) in 5P7.4 was added to a final concentration of 1% (w/v). The remaining steps were performed at room temperature. These SDS-denatured samples were then diluted a further 10-fold with 1% SDS (w/v) in 5P7.4, and the eosin fluorescence emission spectra were collected using a SPEX Fluorolog 3 L-format fluorometer (488-nm excitation wavelength and 500–620-nm emission wavelength; unlabeled ghosts treated as above were used for background subtraction). The total eosin content of the ghost samples was obtained by performing this exact procedure, except omitting the centrifugation of the $C_{12}E_8$-treated membranes. The fractional extraction of band 3 was calculated as the ratio of the eosin fluorescence in the $C_{12}E_8$-extracted membrane supernatant to the total eosin content. Identical results were obtained from using the integrated spectral intensity or the peak eosin fluorescence intensity; ratios obtained from the integrated spectral intensity are reported here with their standard deviations (from triplicate sample extractions and fluorescence measurements).

EPR measurements

X-band (9.8 GHz) EPR and ST-EPR spectra were collected using a Bruker EMX spectrometer equipped with a TM_{110} cavity and with samples contained in 50-μl glass capillaries (VWR Scientific, West Chester, PA). Q-band (34 GHz) spectra were collected using a Bruker ESP-300 spectrometer equipped with a TE_{011} cavity and with samples contained in 0.3-mm i.d. quartz capillaries (Vitro Dynamics, Rockaway, NJ). Sample temperature in both spectrometers was controlled at 37 $\pm$ 0.1°C during data acquisition using standard Bruker variable-temperature units. The effective microwave and modulation fields at the sample were calibrated using peroxylamine disulfonate (Aldrich, Milwaukee, WI) as described previously (Beth et al., 1983). Linear EPR spectra were collected using a peak-to-peak modulation amplitude of 0.5 Gauss and a microwave observer field of $\sim$0.05 Gauss (2 mW at X-band; 0.5 mW at Q-band). V_2' ST-EPR signals (second harmonic out-of-phase absorption) were collected using a peak-to-peak modulation amplitude of 5.0 Gauss and a microwave observer field of $\sim$0.2 Gauss (50 mW at X-band; 7.3 mW at Q-band). The out-of-phase position for detection of the V_2' signal was determined by the self-null method (Thomas et al., 1976). Digital records of all spectra were obtained by signal averaging using standard Bruker data acquisition software.

Analysis of EPR and ST-EPR spectra

Linear EPR spectra were analyzed for determination of principal elements of the A- and g-tensors using a nonlinear least-squares approach based upon the Marquardt-Levenberg method (Hustedt et al., 1993; Hustedt and Beth, 1995). For the case of unconstrained URD, ST-EPR spectra were analyzed using computational approaches described previously (Hustedt and Beth, 1995). For the case of constrained URD, the algorithm described in Hustedt and Beth (2001), which includes the effect of a square-well restriction, was employed. Experimental data were analyzed by incorporating this algorithm into a nonlinear least-squares algorithm, based upon the Marquardt-Levenberg method (Hustedt et al., 1993), and then minimizing the χ^2 statistic between the calculated and experimental spectra. Confidence intervals for each parameter recovered from the experimental data were calculated by holding the parameter of interest constant and allowing the other relevant parameters to vary over their range of possible values.

Delayed fluorescence anisotropy decay measurements

Time-resolved delayed fluorescence anisotropy data from EMA-labeled ghost membranes were collected using a spectrometer that has been described previously (Cobb et al., 1993; Blackman et al., 1996). As in the earlier study, delayed fluorescence was used because the emission dipole is the same as in prompt fluorescence thereby enabling the use of orientation information obtained by fluorescence microscopy. The laser pulse rate was set at 70 Hz, and the PMT was gated during the pulse. Data were collected into 15,360 bins (640 ns wide; total decay time recorded was 9.83 ms). Prompt fluorescence emission was detected at early times, which contam-

inated the delayed fluorescence anisotropy data from 0 to ~20 μs (these data were omitted from the analyses).

Samples were purged of molecular oxygen using procedures described previously (Cobb et al., 1993; Blackman et al., 1996). Sample temperature was controlled by passing water from a refrigerating/heating water bath through the water jacket of the cuvette holder. Erythrocyte ghost samples, prepared by the addition of 50 μl of packed EMA-labeled ghosts to 3 ml of 5P7.4 containing 5 μg/mL phenylmethylsulfonyl fluoride, were equilibrated at 37°C for 15 min in the sample chamber before data collection. Separate decays were recorded every 25 min to verify sample stability and were added together after collection. Anisotropy ($r(t)$) and total intensity ($S(t)$) were calculated as described previously (Blackman et al., 1996).

Analysis of delayed fluorescence anisotropy decays

For a single population of a transmembrane protein undergoing unrestricted URD, the anisotropy decay is predicted to be biexponential (e.g., Szabo, 1984):

$$r(t) = C_0 + C_1 e^{-D_\parallel t} + C_2 e^{-4D_\parallel t}, \quad (6)$$

where $D_\parallel$ is the diffusion coefficient for URD, and C_0, C_1, and C_2 are coefficients that depend on the relative orientation of the absorption and emission dipoles of the probe and the diffusion axis (see definitions in Blackman et al., 1996). The theoretical residual anisotropy in unrestricted URD ($r_\infty^{\text{unrestricted}}$) is equal to the coefficient C_0. Analysis according to this model followed methods described previously (Blackman et al., 1996). The residual anisotropy (r_∞) was also determined by analyzing data according to a multi-exponential decay model, using a Marquardt-Levenberg least-squares algorithm (Beechem et al., 1991; Beechem, 1992):

$$r(t) = \sum_{i=0}^{3} \beta_i e^{-\phi_i t} + r_\infty \quad (7)$$

Three decay components were required to give good fits as judged by χ^2 values and inspection of residual plots.

The effects of a restoring potential on the amplitude of URD were calculated according to two different forms of restriction: a square-well potential (i.e., reflecting barriers) and a harmonic-well potential. Equations describing the anisotropy decay for restricted-amplitude diffusion within a square well are given by Wahl (1975). With this model, the anisotropy decays to a higher r_∞ value which is given by:

$$r_\infty^{\text{restricted}} = C_0 + C_1 \frac{\sin^2(\Delta/2)}{(\Delta/2)^2} + C_2 \frac{\sin^2\Delta}{\Delta^2}, \quad (8)$$

where Δ is the full angular width of the square well. For restriction within a harmonic potential well, r_∞ is given by (derived from Szabo, 1984):

$$r_\infty^{\text{restricted}} = C_0 + C_1 e^{-\langle\gamma^2\rangle} + C_2 e^{-4\langle\gamma^2\rangle}, \quad (9)$$

where $\langle\gamma^2\rangle$ is the mean-squared angular displacement. The effects of these two different potentials on the r_∞ are approximately equivalent for the same mean-squared angular displacements (calculations not shown).

Based upon the relative stoichiometries of band 3 and ankyrin, all copies of band 3 should not be attached to the membrane skeleton via interactions with ankyrin (see Bennett and Stenbuck, 1979; Nigg and Cherry, 1980). Therefore, the r_∞ for intact ghost membranes is treated as a weighted average of two components: one undergoing restricted-amplitude URD (attached to the membrane skeleton) and one undergoing unrestricted URD (unattached):

$$r_\infty^{\text{intact ghosts}} = f r_\infty^{\text{restricted}} + (1 - f) r_\infty^{\text{unrestricted}} \quad (10)$$

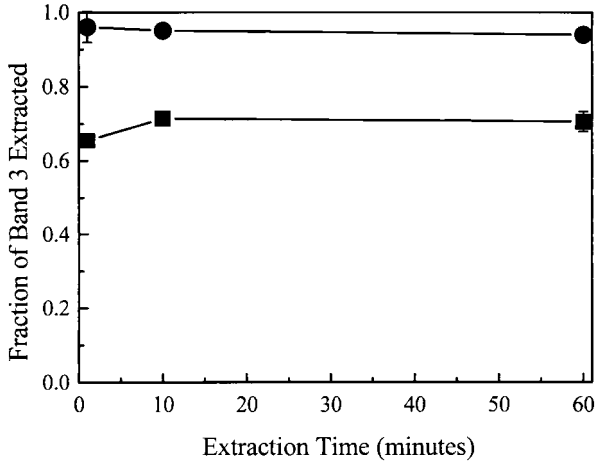

FIGURE 2 Fraction of EMA-band 3 extracted from control and trypsin-treated ghost membranes. The lower points (■) were measured from intact EMA-labeled ghost membranes as described in Materials and Methods. The upper points (●) were obtained from EMA-labeled ghost membranes following cleavage of the cytoplasmic domain of band 3 with trypsin. The data are plotted as the average value of three measurements ± SD.

A value for f (0.28) was assigned based on results from extractability of band 3 from ghost membranes. Using values for the coefficients C_0 (0.017), C_1 (0.047), and C_2 (0.209) from previous confocal microscopy results (Blackman et al., 1996) and a value for $r_\infty^{\text{intact ghosts}}$ from TOA measurements, Eqs. 8, 9, and 10 were used to calculate $r_\infty^{\text{restricted}}$ and the angular restriction. Confidence limits were assigned based upon the 95% confidence level for determination of C_0 (Blackman et al., 1996). In all cases, results from analysis of TOA data using the harmonic-well potential were essentially identical to those for the square-well potential; therefore, only the latter is reported in Results.

RESULTS

Fraction of band 3 interacting with the membrane skeleton

Previous work has indicated that only a fraction of band 3 is extracted from intact ghost membranes by nondenaturing detergents (e.g., Casey and Reithmeier, 1991), with the rest remaining associated with the insoluble membrane skeleton. This observation is consistent with the measurements that have been reported that strongly suggest that the dissociation of band 3 from ankyrin is remarkably slow with a half-time of hours (see Low, 1986; Thevenin and Low, 1990). Therefore, the fraction of band 3 that interacts with the membrane skeleton in intact ghost membranes has been estimated by measuring the fraction that can be extracted at short times (i.e., less than 1 h) by the nondenaturing detergent $C_{12}E_8$ as shown in Fig. 2. In control ghosts, 28% of the total EMA-labeled band 3 remains associated with the membrane skeleton following extraction when using 1% (w/v) $C_{12}E_8$. This value does not change significantly with incubation time in the 1–60-min time window nor with the concentration of detergent in the 0.5–2.0-wt % range. How-

ever, cleavage of the cytoplasmic domain of band 3 with trypsin before extraction leads to release of >95% of the copies of band 3. Therefore, it is reasonable to assume that the interaction of the cytoplasmic domain with the membrane skeleton is largely responsible for the reduced extraction efficiency in control ghost membranes. These data have been employed to obtain a reasonable estimate for the fraction, *f*, of band 3 that interacts with the membrane skeleton. As discussed more fully below, this estimate is required for analyses of the spectroscopic data in terms of an angular restriction to URD.

Predicted effects of constrained uniaxial rotational diffusion on ST-EPR spectra

Fig. 3 shows calculated V_2' ST-EPR spectra that demonstrate the sensitivity of this signal to the amplitude of URD at X- and Q-band microwave frequencies using the orientation of the spin label relative to the URD axis that is appropriate for SL-H_2-DADS-maleimide-labeled band 3. The angles (θ = 37° and ϕ = 61°; see Hustedt and Beth, 2001, for definition of angles) were obtained from the analysis of labeled band 3 in intact erythrocytes oriented by flow (Hustedt and Beth, 1996) and were also those that gave the best fit of X-band V_2' ST-EPR spectra to an unconstrained URD model (see Fig. 9 of Hustedt and Beth, 1995). For the case of a square-well angular potential and a single diffusing species, it is apparent that the V_2' signal is highly sensitive to the amplitude of URD for angular excursions of less than 60° (full-width) for both microwave frequencies with this probe geometry. In the range from 60° to 90°, there is limited sensitivity to the amplitude of URD, and for angles larger than 90°, there is almost no sensitivity to the amplitude of motion. This sensitivity is shown graphically in Fig. 4 where the ratio parameters are plotted versus Δ, the full-width of the square-well potential. A thorough discussion of the sensitivity of ST-EPR spectra to Δ for a variety of labeling geometries and as a function of relevant spectrometer variables is provided in Hustedt and Beth (2001).

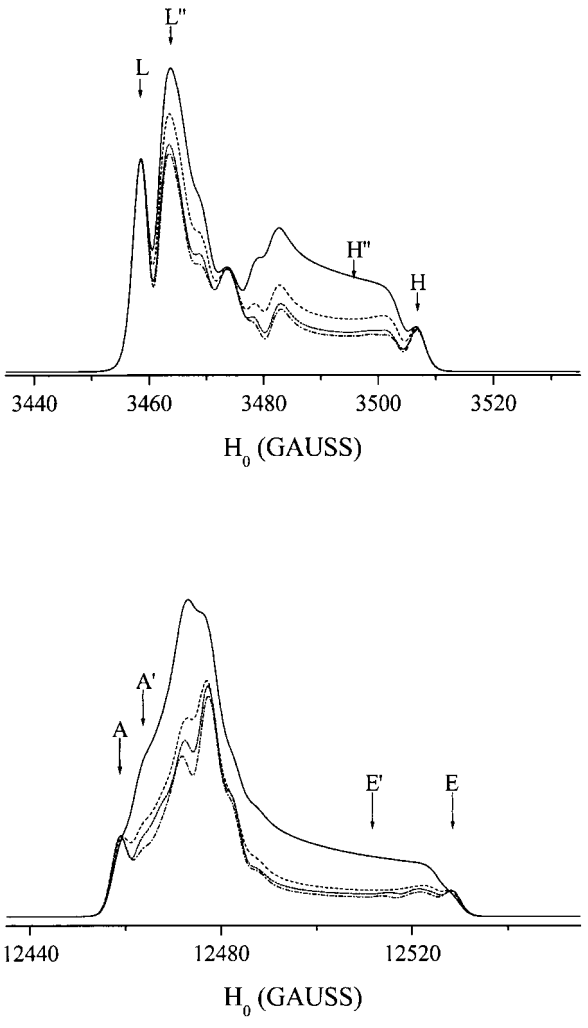

FIGURE 3 Calculated V_2' ST-EPR spectra at X-band (*top*) and at Q-band (*bottom*) for a restricted amplitude URD model. Each panel shows spectra calculated for Δ = 1° (*solid line*), Δ = 30° (*dashed line*), Δ = 60° (*short dashed line*), and Δ = 90° (*dot-dash line*). The spectra were calculated at 50-kHz Zeeman field modulation frequency, τ = 15 μs, θ = 37°, and ϕ = 61° using a microwave observer field of 0.2 Gauss. The field positions where spectral amplitudes that are sensitive to Δ are measured are shown superimposed on the calculated spectra at X- and Q-band.

Effects of trypsin cleavage on ST-EPR spectra from spin-labeled band 3

Previous studies showed that the TOA decays observed from EMA-labeled band 3 were significantly altered following cleavage with trypsin near the cytoplasmic membrane surface (Nigg and Cherry, 1980). However, it has remained uncertain how much of this change in TOA decay was due to release of a restriction in the amplitude of motion of the transmembrane domain versus dissociation of large clusters of band 3 as discussed previously (Blackman et al., 1998a) and in subsequent sections of this work. Given the ability to carry out studies of rotational motion by ST-EPR and the development of computational tools to analyze data in terms of restricted-amplitude URD, the effects of trypsin cleavage on the V_2' signal were characterized as shown in Fig. 5. It is immediately clear from these experimental data that cleavage of the link with the cytoplasmic domain results in only subtle changes in the ST-EPR spectra at either X- or Q-band microwave frequency (compare upper and lower spectra in each column). The results of analyses based upon two different models are shown superimposed on the experimental data in Fig. 5. In the first model, it is assumed that all copies of band 3 undergo unrestricted URD both in control and in trypsin-treated membranes. Simultaneous fitting of the two spectra from control ghosts (upper row) results in a best-fit recovery (based upon minimization of

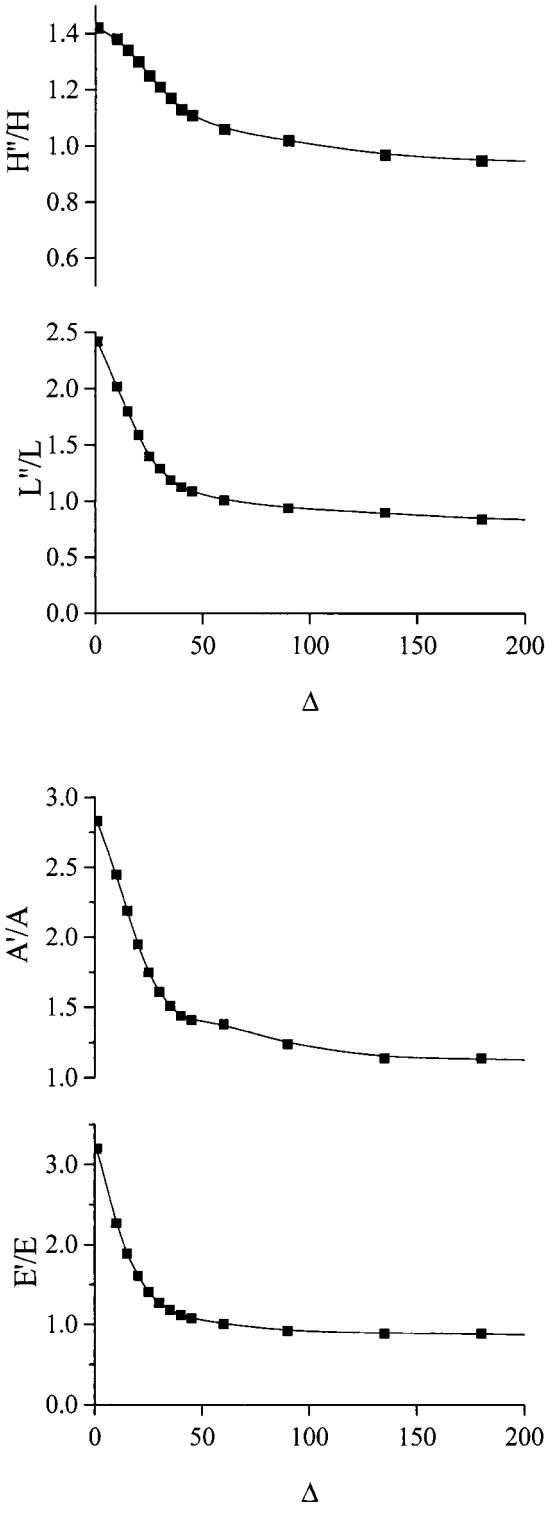

FIGURE 4 Spectral sensitivity plots for V_2' ST-EPR spectra as a function of the width of the restriction potential. The ratios of spectral amplitudes (defined in Fig. 3) are plotted versus Δ for the spin label orientation that has been determined for band 3 ($\theta = 37°$, $\phi = 61°$) at X-band (9.8 GHz, *upper*) and Q-band (34.0 GHz, *lower*) microwave frequencies. The additional spectra from which the ratios were measured (not shown) were calculated using the same parameters listed in the legend to Fig. 3.

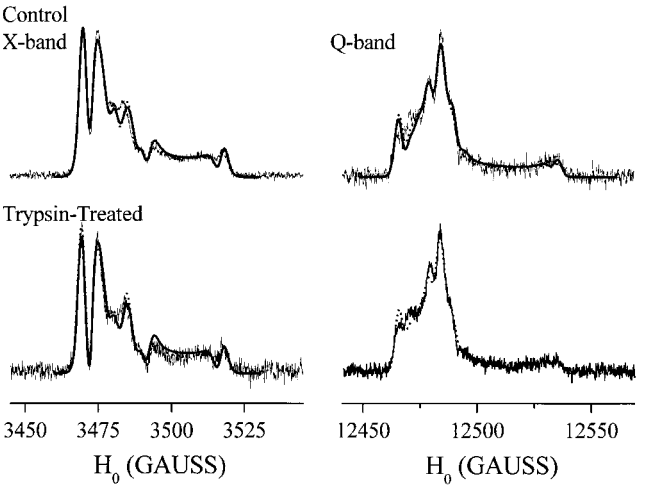

FIGURE 5 V_2' ST-EPR data and best-fit simulations obtained from control and trypsin-treated erythrocyte ghost membranes. The experimental spectra from control (*upper row*) and trypsin-treated (*lower row*) ghost membranes are shown as fine solid lines. The two spectra in the left column were obtained at X-band (9.8 GHz), and the two spectra in the right column were obtained at Q-band (34.0 GHz) using the instrument parameters given in Materials and Methods. Two different analyses are shown superimposed on the experimental data. The solid heavy lines are the simultaneous best fit (minimum χ^2) of the X- and Q-band spectra in each row to an unconstrained URD model: $\tau = 6$ μs (control) and $\tau = 12$ μs (trypsin treated). For these calculations, T_{1e}, T_{2e}, and the Gaussian post-broadening were allowed to vary between the X- and Q-band spectra while τ was constrained to be the same for each. The dotted lines are the simultaneous best fit (minimum χ^2) of the X- and Q-band spectra in each row to a constrained URD model: $\tau = 8$ μs and $\Delta = 322°$ (control); $\tau = 7$ μs and $\Delta = 318°$ (trypsin treated). For these calculations, T_{1e}, T_{2e}, and the Gaussian post-broadening were allowed to vary between the X-and Q-band spectra while τ and Δ were constrained to be the same for each. X-band spectra are 100 Gauss in width, and the Q-band spectra are 120 Gauss in width.

χ^2) of 6 μsec for the correlation time for URD. The same analysis of the two spectra from trypsin-treated membranes (lower row) results in recovery of 12 μs for the correlation time. At the 95% confidence level, these values are not statistically different. In both cases, this model yields a good fit of the experimental data. In the second model, it is assumed that all copies of band 3 undergo restricted-amplitude URD. Reanalysis of the two spectra in the upper row results in recovery of a correlation time of 8 μs and a square-well restriction of 322° whereas the lower spectra yield 7 μs and 318°. At the 95% confidence level, neither the correlation time nor Δ are significantly different for the two preparations.

The spectra in Fig. 5 have also been analyzed using a model where there are two populations: one undergoing unrestricted URD and the second one undergoing restricted-amplitude URD as shown in Fig. 6. Best-fit values of χ^2 are shown as a function of the fraction of the restricted component for different values of the width of the square-well restriction, Δ, at X-band (upper) and at Q-band (lower) microwave frequencies. The horizontal solid line defines

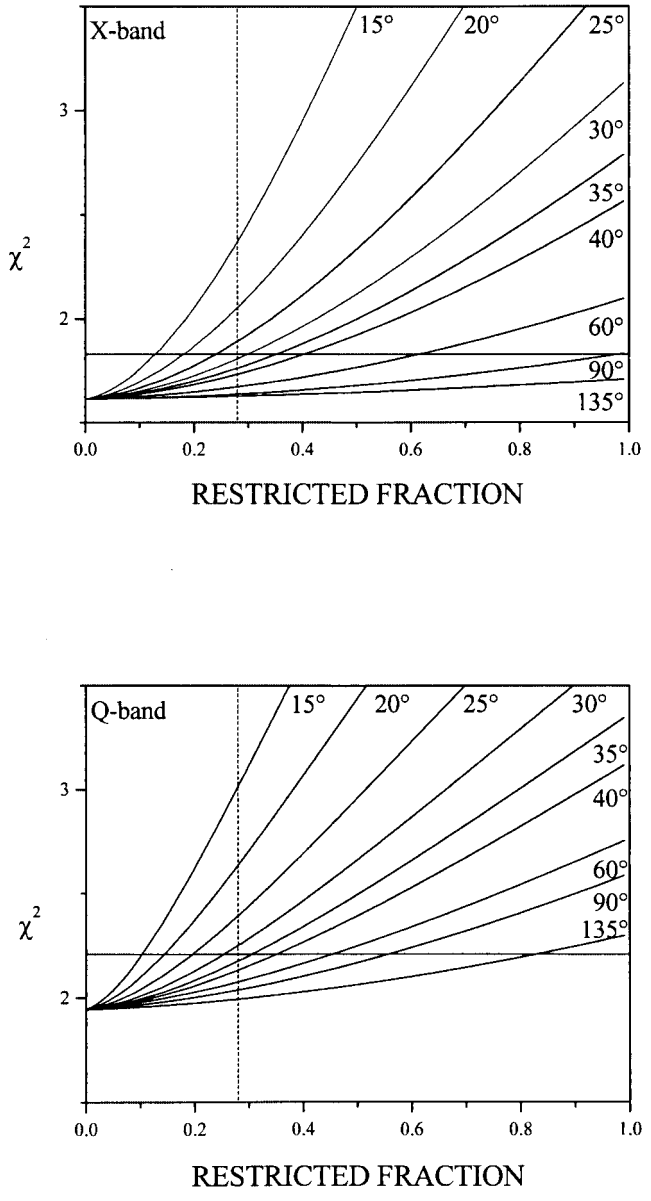

FIGURE 6 Sensitivity of V_2' ST-EPR spectra to the fraction of rotationally restricted band 3. The family of curves in the upper panel was calculated at X-band microwave frequency using the indicated values for the width of the square-well restriction (Δ), and the family of curves in the lower panel was calculated at Q-band microwave frequency. The horizontal line indicates the 95% confidence interval for detection of a change in the ST-EPR spectrum following trypsin cleavage. The vertical dashed line at 0.28 restricted fraction denotes the experimentally determined fraction of membrane skeleton bound band 3. The χ^2 values (ordinate) were calculated by statistical comparison with the experimental data shown in Fig. 5.

the 95% confidence level for discriminating between this two-component model and a one-component model where all copies undergo unrestricted URD. The data in Fig. 6 show that at small values of Δ, very small restricted fractions can be detected and that as Δ increases, increasing restricted fractions are necessary for detection. Fig. 6 also

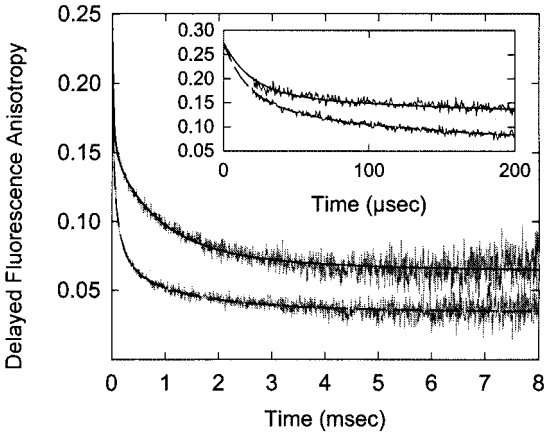

FIGURE 7 Time-resolved delayed fluorescence anisotropy data from control and trypsin-treated erythrocyte membranes. Data are shown for intact membranes (upper decay; fit is *solid line*) and trypsin-treated membranes (lower decay; fit is *dashed line*). For display, the 15,360 data points were run-averaged with a 9-point (5.76-μs) window; fits were performed on un-averaged data. (*Inset*) The first 200 μs of the same data and fits, displayed without run-averaging. Data for control and trypsin-treated membranes were simultaneously fit to a sum-of-exponentials model (Eq. 7) in which the residual anisotropy term, r_∞, was allowed to vary. Fit results are, for control (χ^2 = 0.98), decay constants 20 μs, 150 μs, and 1216 μs; amplitudes 0.065, 0.035, and 0.074; and r_∞ = 0.066; for trypsin (χ^2 = 0.98), decay constants 35 μs; 196 μs, and 1458 μs; amplitudes 0.092, 0.056, and 0.033; and r_∞ = 0.035.

shows that for the spin-label orientation determined for band 3, Q-band is more sensitive than X-band for detecting a small restricted fraction.

Determination of the minimum constraint to URD depends directly upon the fraction of band 3 that is linked to the membrane skeleton. Studies on detergent solubilization of band 3 from intact ghost membranes have indicated that 28% of band 3 is not readily extractable by nondenaturing detergents, due to the interaction of this subpopulation with the membrane skeleton (Fig. 2). Even if 72% of the copies of band 3 exhibit unrestricted URD and 28% were restricted to diffuse in a square well of less than 32° full width, this would be detectable in the ST-EPR data at Q-band following cleavage with trypsin at the 95% confidence level as shown in Fig. 6, lower. These ST-EPR results establish a lower-limit on the amount of restriction imposed even though they do not permit an absolute determination of the value of Δ.

Calculation of the amplitude of rotational diffusion from delayed fluorescence anisotropy data

Fig. 7 shows time-resolved delayed fluorescence anisotropy data for EMA-labeled band 3 in intact ghost membranes and in trypsin-treated ghost membranes. As has been previously shown (Nigg and Cherry, 1980), cleavage with trypsin

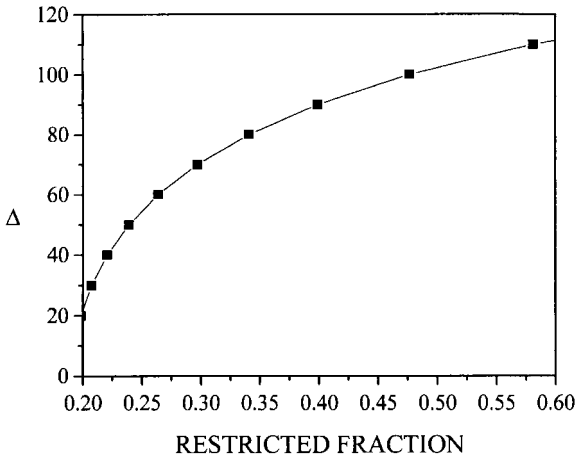

FIGURE 8 Dependence of Δ on the fraction of restricted band 3. Values of *f*, the restricted fraction, were calculated for given values of Δ (Eq. 10) using $r_\infty^{\text{intact ghosts}} = 0.066$, $r_\infty^{\text{unrestricted}} = 0.017$; values of $r_\infty^{\text{unrestricted}}$ were calculated from Eq. 8, and C_0 (0.017), C_1 (0.047), and C_2 (0.209) from previous work (Blackman et al., 1996).

produces a large increase in the apparent rotational mobility of band 3, as reflected in the decrease of the delayed fluorescence r_∞ from 0.066 to 0.035. Analyses of these data according to a phenomenological sums-of-exponentials model (Eq. 7) shows that cleavage with trypsin increases the relative amount of an apparent fraction of rapidly rotating band 3, and decreases the relative amount of an apparent fraction of slowly rotating band 3. The same results, including an r_∞ of 0.035, were obtained in previous work when the data were analyzed according to a multiple-population URD model (Eq. 6) (Blackman et al., 1996). The fastest apparent decay time is consistent with what would be expected for a small oligomer of band 3 such as an unrestricted dimer or tetramer (Matayoshi and Jovin, 1991) and is also reasonably consistent with the rotational correlation time determined in ST-EPR studies (Fig. 5) (see also Hustedt and Beth, 1995).

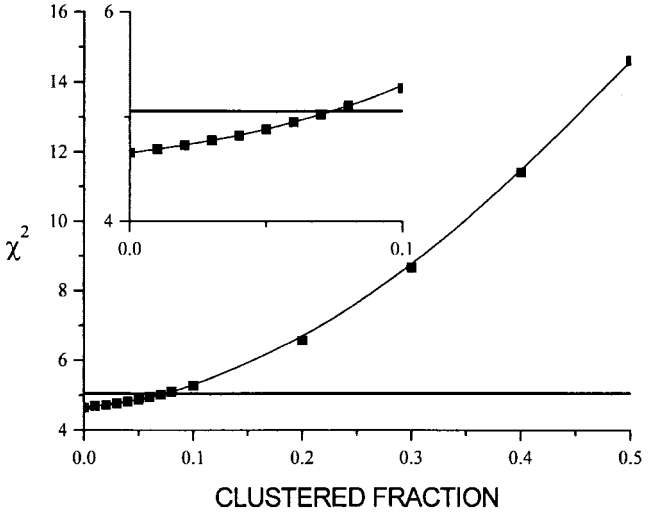

FIGURE 9 Effect of a highly clustered fraction of band 3 on fitting experimental ST-EPR data. The experimental ST-EPR spectra from control ghosts obtained at X- and Q-band microwave frequencies (upper row of Fig. 5) were simultaneously fit to a two-component model where one component exhibited unconstrained URD and the second component was immobilized on the ST-EPR timescale ($\tau = 10$ ms). The χ^2 values on the ordinate represent the best fits of this two-component model that were obtained by allowing the correlation time for the unrestricted component to float in the calculation. The solid horizontal line is the 95% confidence level for discriminating between this two-component model and a single unrestricted URD model.

The r_∞ values for EMA-labeled ghosts have been interpreted in this work in terms of a square-well restriction on the amplitude of URD for that subpopulation of band 3 that is linked to the membrane skeleton. As outlined in Materials and Methods, prior knowledge of the orientation of the EMA probe relative to the membrane normal axis (Blackman et al., 1996) enables prediction of the delayed fluorescence r_∞ for band 3 undergoing unrestricted URD. The value for C_0 corresponds to the appropriate value for $r_\infty^{\text{unrestricted}}$ of 0.017. The higher residual anisotropy of 0.066 in intact ghost membranes ($r_\infty^{\text{intact ghosts}}$) minimally reflects contributions from freely rotating band 3 ($r_\infty^{\text{unrestricted}}$) and from rotationally hindered band 3 ($r_\infty^{\text{restricted}}$) as given in Eq. 10. As in the ST-EPR studies, it is necessary to know the fraction of rotationally hindered band 3 for calculation of the square-well restriction. Using the value of 28% determined in this work (Fig. 2), Eq. 10 yields a value for $r_\infty^{\text{restricted}}$ of 0.175. Using this value for $r_\infty^{\text{restricted}}$ and the previously determined values for C_0, C_1, and C_2, Eq. 8 yields a full angular restriction width of 73° for a square-well potential (95% confidence interval of 43–106°). In carrying out these analyses of the TOA data, the predicted value for $r_\infty^{\text{unrestricted}}$ (0.017) has been employed even though a value for r_∞ of 0.035 was determined from fitting experimental delayed fluorescence data following trypsin cleavage (Fig. 7). Possible explanations for experimental observation of the modestly higher value and alternative interpretations of the TOA results are presented in the Discussion below.

DISCUSSION

Overview of previous work

A large body of previous work has led to definition of interactions between the cytoplasmic domain of band 3 and a number of peripheral membrane proteins including ankyrin (see Low, 1986). The working model that has emerged from these studies is that there is a population of band 3 dimers that do not interact with ankyrin and there is a second population of tetramers that interact with ankyrin and thereby form a link with spectrin, the major protein comprising the membrane skeleton that lines the cytoplasmic membrane surface in human erythrocytes (Low, 1986;

Hall and Bennett, 1987; Michaely and Bennett, 1995). Protein 4.2 also interacts with the cytoplasmic domain of band 3, and it has been proposed that this interaction strengthens the interaction between band 3 and ankyrin (Rybicki et al., 1996). The importance of the physical link between band 3 and the membrane skeleton, with regards to erythrocyte shape, viscoelastic properties, and stability, has been demonstrated by Peters et al. (1996) and by Southgate et al. (1996) in studies of murine erythrocytes completely deficient of band 3. In both studies, there appeared to be a normally assembled membrane skeleton, but the erythrocytes were small, spherocytic, and fragile. Interestingly, even a 20% reduction in the number of copies of band 3 has been reported to result in a similar phenotype (Lux and Palek, 1995). Recent data further suggest that ~20% of cases of hereditary spherocytosis involve alterations in the level or composition of band 3 (reviewed in Tanner, 1997).

Given the importance of the interaction between the lipid bilayer and the membrane skeleton that is mediated by band 3, it has been of considerable interest to determine the mechanical properties of the linkage and, ultimately, how these properties contribute to membrane stability and to cell shape. One way to address the dynamic flexibility of the linkage is to study the rotational diffusion of the transmembrane domain of band 3 both with and without the cytoplasmic domain attached. A reasonable initial model would be to assume that the transmembrane domain undergoes URD due to the anisotropic constraints of the lipid bilayer as reported in the ST-EPR studies of Hustedt and Beth (1995). That population of band 3 not bound to the membrane skeleton by ankyrin would undergo unconstrained URD whereas that population that binds ankyrin and, therefore, indirectly linked to the orthogonally arranged spectrin meshwork, would undergo constrained URD. The amplitude of URD for the bound population of band 3 would be dependent in large part on the mechanical properties of the segment of the cytoplasmic domain between the ankyrin-binding site and the transmembrane domain. Based upon this simple two-state model, one would predict that the major effect of cleavage of the cytoplasmic domain with trypsin would be to release the constraint to URD so that all copies would undergo unconstrained URD. Although this may be an oversimplified model for band 3 in the erythrocyte membrane and for the true nature of band 3-ankyrin interactions (see Low, 1986; Matayoshi and Jovin, 1991; Blackman et al., 1996; Zhang et al., 2000, for further discussions), it does permit the interpretation of major features of the spectroscopic data from studies of band 3 rotational diffusion in terms of known and reasonably well-characterized protein-protein interactions. Although the spectrin network itself may exhibit some local flexibility when interacting with the membrane, and its coupling to the cytoplasmic domain of band 3 via ankyrin also may allow some flexibility, large-amplitude rotational motions of these proteins in the micro- to millisecond time scale are not likely due to the multiple contacts involved in the known protein-protein interactions. Clearly, detailed studies of the dynamic flexibility of spectrin and ankyrin while assembled with band 3 in ghost membranes would be required to determine their contributions to the rotational mobility of the transmembrane domain of band 3. However, in the absence of these exact data, it is not unreasonable to assign the majority of the flexibility observed to the cytoplasmic domain of band 3 given the large body of previous work.

Previous studies have provided indications that the cytoplasmic domain of band 3 is reasonably flexible. Perhaps the most compelling evidence was provided in the work of Wang et al. (1993) on two-dimensional crystals of band 3. Two different crystal forms were obtained that differed primarily in the orientation of a small subdomain with respect to the major transmembrane core. This subdomain was postulated to be the proximal portion of the cytoplasmic domain, and hence, these data strongly suggested that this segment of the cytoplasmic domain can exist in at least two different conformations that differed by ~60° in their orientation relative to the transmembrane domain. Though these static measurements did not provide any direct evidence for inter-conversions between these two conformations under normal conditions (i.e., in the absence of crystal packing interactions), they did provide strong indications that this segment of band 3 can exhibit two different structures in a crystalline array.

Early studies suggested that the cytoplasmic domain of band 3 might be elongated, exhibiting an axial ratio of ~10:1 (estimated dimensions of 25 × 250 Å; Low et al., 1984) and that the N-terminus extends into the interior of the erythrocyte (Weinstein et al., 1978). Though circular dichroism studies have indicated significant α and β secondary structure (Oikawa et al., 1985), this large axial ratio, coupled with the presence of some random coil structure (Oikawa et al., 1985), suggests that portions of the cytoplasmic domain could exhibit considerable conformational flexibility. This is also supported by recent work on the structure of the cytoplasmic domain of band 3 where, in the crystal structure determined at low pH, the N- and C-terminal portions are poorly defined, presumably due to lack of ordering even in the crystalline state (Zhang et al., 2000). The ankyrin-binding site has been localized to two regions of the cytoplasmic domain (Willardson et al., 1989). Residues in the central portion of the primary structure as well as residues in the acidic N-terminus have been implicated in ankyrin binding. The few studies of dynamics that have been reported do provide hints of a flexible structure, particularly in the acidic N-terminal region that comprises a portion of the ankyrin-binding site. For example, fluorescence experiments have demonstrated the existence of multiple conformations and the effects of pH on their equilibrium distribution (reviewed in Low, 1986). Time-resolved phosphorescence experiments using an antibody to the cytoplasmic domain indicated a highly flexible structure in the

region of the binding site (McPherson et al., 1992). ST-EPR studies of spin-labeled hemoglobin (Cassoly, 1982) and spin-labeled glyceraldehyde-3-phosphate dehydrogenase (Beth et al., 1981) bound to the N-terminus of the cytoplasmic domain also suggested that there was considerable motional freedom of this region relative to the hindered rotation of the transmembrane domain.

Previous TOA studies, including the seminal work by Nigg and Cherry (1980), demonstrated that cleavage with trypsin produced marked changes in the anisotropy decay of EMA-labeled band 3, one of the most obvious changes being a substantial reduction in r_∞. At that time, it was not possible to assign the reduction in r_∞ to a change in a specific dynamic process or to any structural rearrangement. Specifically, the reduction in r_∞ could have resulted from a change in orientation of the absorption or emission dipoles of EMA with respect to the URD axis, from a dissociation of large clusters of band 3 that were immobile on the millisecond time scale, from a release in a constraint to URD, or from a combination of these possibilities. Since this early work, Blackman et al. (1996) showed that cleavage with trypsin does not alter the orientation of the fluorescence absorption and emission dipoles of EMA based upon direct evidence from polarized fluorescence confocal microscopy data obtained on single ghost membranes. Blackman et al. (1998a) subsequently showed that cleavage with trypsin does not alter the distribution of oligomeric species of EMA-labeled band 3 in ghost membranes as reported by fluorescence resonance energy homotransfer. Having eliminated these two potential explanations, the most likely remaining explanation for the reduction in r_∞ is the release of a partial constraint to rotational diffusion, which is consistent with the known interaction of the cytoplasmic domain of a significant subpopulation of band 3 oligomers with ankyrin and, thereby, with the membrane skeleton. Given this body of previous work, it is possible to quantitate the rotational flexibility of the cytoplasmic domain by obtaining a reasonable estimate for the fraction of band 3 that interacts with the membrane skeleton.

Estimation of the fraction of band 3 that is bound to the membrane skeleton

Early studies on the interactions between ankyrin and the cytoplasmic domain of band 3 suggested that the dissociation rate was very slow (half time in the hours range; see Low, 1986). These data, combined with the observation that only a fraction of band 3 can be extracted from intact ghost membranes when using nondenaturing detergents (see Casey and Reithmeier, 1991), suggested that it is the subpopulation of band 3 that is interacting with the membrane skeleton that resists extraction. This simple model was tested by cleaving the cytoplasmic domain of band 3 with trypsin before detergent extraction as shown in Fig. 2. These data clearly showed that by cleaving the link between the transmembrane and cytoplasmic domains, the transmembrane domain became nearly completely extractable. If tetramers of band 3 serve as the ankyrin-binding site and all copies of ankyrin that are present in ghost membranes participate in band 3 interactions, these data suggest that there are ~7% as many copies of ankyrin present as band 3 based upon 28% being resistant to extraction in control ghosts. This number is in reasonable agreement with the predicted stoichiometry from densitometric scans of SDS-PAGE gels that have suggested 10% to 15% as many copies of ankyrin as band 3 (Fairbanks et al., 1971). Given the reasonable agreement between the previous estimates of relative abundance of ankyrin and the current estimate in Fig. 2, it is reasonable to assign the detergent-resistant fraction as being that fraction that is involved in interactions with the membrane skeleton in intact ghost membranes. These results and interpretations are entirely consistent with previous studies by Yi et al. (1997) on ankyrin-deficient nb/nb mice. Specifically, this work showed that in control erythrocytes, 28% of band 3 was not readily extractable, but in ankyrin-deficient erythrocytes, 92% of band 3 was extracted with $C_{12}E_8$.

Interpretation of ST-EPR results

Previous ST-EPR studies have shown that the rotational diffusion of the transmembrane domain of band 3 is characterized by URD about the membrane normal axis (Hustedt and Beth, 1995). A major finding from the present studies is that cleavage of the cytoplasmic domain with trypsin does not lead to any detectable changes in the ST-EPR spectra of SL-H_2-DADS-maleimide-labeled band 3 in ghost membranes. Using the computational algorithm developed in Hustedt and Beth (2001), it is possible to interpret this result based upon the sensitivity of ST-EPR to the amplitude of URD and upon the fraction of band 3 oligomers that interact with the membrane skeleton. Taking the value of 28% for the fraction of band 3 that is involved in binding to the membrane skeleton and making the assumption that the motional restriction imposed on the transmembrane domain limits Δ to less than 32°, then the Q-band ST-EPR spectrum would indicate apparent faster rotational motion upon cleavage with trypsin (Fig. 6, lower panel). However, the failure to observe any significant change indicates that the amplitude of URD in the restricted fraction is greater than this value. If the fraction of band 3 that interacts with ankyrin is greater than 28%, then slightly greater sensitivity to angles larger than 32° would be predicted. Conversely, if the fraction is less than 28%, somewhat less sensitivity would be predicted as demonstrated in Fig. 6. What is absolutely clear is that if there were a rigid motional coupling between the two domains of band 3 that limited motional excursions of the transmembrane domain to less than 15°, then there would be significant changes in the ST-EPR spectra following cleavage with trypsin if

greater than 10% of band 3 was bound to ankyrin. The predicted sensitivity of the V_2' ST -EPR signal as a function of the fraction of band 3 bound to ankyrin is shown graphically in Fig. 6 for selected motional restrictions along with the 95% confidence level for detecting the bound fraction.

The calculations shown in Fig. 6 demonstrate that Q-band is more sensitive than X-band for detecting weak restrictions to URD of band 3. This is due, in large part, to the orientation of the spin label relative to the URD axis. Specifically, when the nitroxide *z* axis is aligned, or in this case nearly aligned ($\theta = 37°$), with the diffusion axis, then motion does not lead to a large change in resonance condition because it is the nitroxide *x* and *y* axes that are being interconverted (see Beth and Robinson, 1989, for an extensive discussion of this topic). Microwave frequencies lower than X-band would be even less sensitive for this geometry. At Q-band, the spectral dispersion due to the g-anisotropy of the nitroxide is large enough (comparable to the A-anisotropy) to lead to significant sensitivity to motional averaging of the nitroxide *x* and *y* axes and hence, there is reasonable sensitivity to the width of the restriction. A priori, it might be predicted that microwave frequencies even greater than Q-band would give even greater sensitivity to large values of Δ. However, as shown in Hustedt and Beth (2001), and as discussed previously (Beth and Robinson, 1989), the magnetic anisotropy is not the sole determinant of spectral sensitivity to rotational motion when detecting the conventional V_2' signal in ST-EPR. The calculated spectra in Hustedt and Beth (2001) demonstrate that W-band (94 GHz) does not provide increased sensitivity to larger values of Δ than Q-band. However, it remains to be explored whether W-band spectra will offer some distinct advantages with regard to determination of Δ in the $0-60°$ range and, in particular, for very strong constraints to URD, and with regard to improved sensitivity for some probe orientations.

Interpretation of TOA results

The data in Fig. 7 show that there are substantial changes in the anisotropy decay, particularly the r_∞, following cleavage with trypsin. As discussed above, a likely explanation for the majority of this change in r_∞ is the release of a constraint to URD. The analytical expressions that relate r_∞ to the width of the restricting potential, which were developed in Materials and Methods, can be employed to interpret these TOA data as described in Results. Two approximations must be made to calculate a restriction from the observed change in r_∞. First, the fraction of band 3 that interacts with the membrane skeleton must be estimated based upon available data. As shown in Results, a reasonable estimate for this fraction is 28% (Fig. 2). Second, the data have to be interpreted based upon a realistic model. A simple two-state model has been chosen based upon known protein-protein interactions as discussed above. Clearly, the erythrocyte membrane is a complex assembly of proteins and lipids and there are many potential interactions between band 3 and other proteins that are not accounted for in a two-state model. For example, there are several reports of interactions between band 3 and glycophorin A that could contribute to some extent to the effective size of some band 3 oligomers in situ (Che and Cherry, 1995; reviewed in Tanner, 1997). In addition, it has been reported in one study that band 4.2 can bind both to the cytoplasmic domain of band 3 and to spectrin (Golan et al., 1996). Such an interaction could lead to a second way of forming a link between band 3 and the membrane skeleton.

One aspect of the analysis of TOA data to determine the constraint on URD merits discussion. Specifically, following trypsin cleavage, the r_∞ observed experimentally was 0.035. The value for r_∞ predicted from the measured value for C_0 is 0.017 (95% confidence interval of 0.001–0.033; Blackman et al., 1996) making the assumption that all copies of band 3 undergo unrestricted URD following cleavage with trypsin. In the absence of any changes in the orientation of the absorption and emission dipoles of EMA following trypsin cleavage (Blackman et al., 1996), there are three straightforward ways to explain this small difference.

First, a residual constraint to URD following scission of the linkage with the cytoplasmic domain could give this result. If this constraint was imposed on all copies of band 3, Eq. 8 can be used to calculate a weak restriction of 186° for a square-well potential. However, there are currently no data to suggest that a residual restriction to URD should exist in terms of known protein-protein interactions.

Second, a small population of highly immobilized band 3 (on the 10-ms time scale) would raise the r_∞. Using Eq. 10, and the values for r_∞ for the two components, an immobilized or highly clustered fraction comprising 9% (95% confidence interval of 1–16%) of the total would be required to increase the predicted residual anisotropy (0.017) to that observed experimentally (0.035). In this calculation, a residual anisotropy of 0.210 for clustered band 3 has been used based upon previous studies that include the effects of resonance energy homotransfer (Blackman et al., 1998a). A 9% immobilized fraction is not incompatible with the resonance energy homotransfer studies of Blackman et al. (1998a). Specifically, these studies were consistent with 0–16% of the copies of band 3 being clustered to some extent depending on the model chosen for analyzing the homotransfer data. Other studies have suggested that small-scale clustering of membrane proteins, including band 3, is a normal consequence of erythrocyte aging and that this may serve as a signal for cell senescence (e.g., Turrini et al., 1991; Corbett and Golan, 1993). Given that there are data that suggest the existence of a small fraction of clustered band 3, it is reasonable to assign at least a portion of the small discrepancy between the observed and predicted r_∞ to the presence of this population. If the fractions of restricted and free band 3 are reduced proportionally and the r_∞ for

clustered band 3 is taken, then an $r_\infty^{\text{restricted}}$ of 0.139 is calculated. This corresponds to a square-well restriction width of 90°. Thus, by this model, two-thirds of band 3 undergoes unconstrained URD, one-fourth undergoes restricted URD of 90° amplitude, and 9% is immobilized. The important point to emphasize is that the two-state model described in Results, and this three-state model that includes a 9% fraction of highly clustered band 3, both predict a highly flexible linkage. An argument against the existence of a 9% population of clustered band 3 is provided by the ST-EPR studies. As shown in Fig. 9, when the V_2' signals from intact ghosts in Fig. 5 (left column) are analyzed in terms of two components, one undergoing unrestricted URD and a second one immobilized on the millisecond time scale, the fits are not as good (higher χ^2) when there is even 2–3% of an immobilized component present. However, on a statistical basis, it is not possible to rule out as much as 8% of band 3 being highly clustered as shown by the 95% confidence level in Fig. 9. A unique aspect of ST-EPR is that sensitivity to very slowly rotating species is high due to the increase in amplitude of this signal as a function of an increase in rotational correlation time (i.e., the signal from immobilized band 3 would be much larger than the signal from rotationally mobile band 3 at the same concentration; see Hustedt and Beth (2001) for additional discussion of this point).

Third, incomplete cleavage of band 3 by trypsin could also result in a higher value for r_∞. SDS-PAGE separation of erythrocyte membrane proteins following treatment with trypsin routinely yields residual Coomassie blue staining in the band 3 monomer region that is 5–10% of the intensity observed in control ghost membranes before trypsin treatment (data not shown). If the population of band 3 that is resistant to trypsin treatment is that population bound to ankyrin, then r_∞ would be increased in direct proportion to the uncleaved fraction. Interestingly, if it assumed that 10% is uncleaved, that this population is bound to ankyrin with an $r_\infty^{\text{restricted}}$ of 0.175, and that $r_\infty^{\text{unrestricted}}$ is 0.017, then an r_∞ of 0.033 is predicted following trypsin cleavage. This is remarkably close to the value of 0.035 determined experimentally. Though not directly tested in the current experiments, it is not unreasonable to hypothesize that the population of band 3 tetramers complexed with ankyrin would be the most resistant to cleavage by trypsin due to restricted access to lysine 360. The important point to be made is that because the width of the square-well restriction was calculated based upon the predicted value for r_∞, incomplete cleavage does not change the value obtained (73°) from the two-state model described in Materials and Methods. In theory, it should be possible to increase the concentration of trypsin and thereby achieve complete cleavage of band 3. However, this results in progressive cleavage of other membrane proteins and to an increase in r_∞ , presumably due to clustering/aggregation of the transmembrane core of band 3 (Nigg and Cherry, 1980). In the final analysis, it may be that both a small amount of clustering and incomplete cleavage of band 3 by trypsin contribute to the higher experimentally measured value for r_∞.

There are features of the TOA results following cleavage with trypsin that require more complicated models to explain. For example, anisotropy decays in the 100-μs to millisecond time window persist after cleavage with trypsin. It is possible that some of the decay components in this time window arise from segmental and/or off-axis motions of band 3 in the membrane (Matayoshi and Jovin, 1991) and that these motions do not respond in a predictable way to cleavage of the cytoplasmic domain with trypsin. A complete explanation of all of the features of the TOA decays is not practical based upon available data. However, the present studies provide an interpretation of rotational dynamics data from two complementary techniques that is physically reasonable based upon current knowledge of the interactions between the major erythrocyte membrane proteins.

Comparison of results from ST-EPR and TOA

The current studies have provided an internally consistent interpretation of rotational diffusion data from two complementary spectroscopic techniques. Initially, it was confusing that TOA yielded a substantial change in anisotropy decay following trypsin cleavage of the cytoplasmic domain whereas the ST-EPR lineshapes were not altered by the same treatment. The development of a computational algorithm to quantitate the effects of constrained URD on ST-EPR spectra clarified this apparent conflict. By establishing the limits of sensitivity of ST-EPR for detecting any constraints to motion under different experimental conditions, it was possible to establish a lower limit on the amount of motional constriction that this interaction imposes on the transmembrane domain. It is clear that if this restriction is sufficiently weak to allow motional excursions in excess of 32°, then ST-EPR will not be sensitive to cleaving the cytoplasmic linkage. The estimate of a rotational restriction width of 73° $\pm$ 30° from the TOA studies is entirely consistent with the absence of changes in the ST-EPR data.

The current studies have provided evidence for a remarkably flexible linkage between the transmembrane domain of band 3 and the segment of the cytoplasmic domain between the cytoplasmic membrane surface and the ankyrin-binding site. It remains an important objective to determine how essential this flexibility is in providing the unique mechanical properties of the erythrocyte membrane.

We thank Drs. David Piston and Hassane Mchaourab (Vanderbilt University) for critiquing the manuscript before submission.

This work was supported by grant R37 HL34737 from the National Institutes of Health.

REFERENCES

Beechem, J. M. 1992. Global analysis of biochemical and biophysical data. *Methods Enzymol.* 210:37–54.

Beechem, J. M., E. Gratton, M. Ameloot, J. R. Knutson, and L. R. Brand. 1991. The global analysis of fluorescence and anisotropy decay data: second-generation theory and programs. *In* Topics in Fluorescence Spectroscopy, Vol. 2: Principles. J. R. Lakowicz, editor. Plenum Press, New York. 241–305.

Bennett, V., and P. J. Stenbuck. 1979. The membrane attachment protein for spectrin is associated with band 3 in human erythrocyte membranes. *Nature.* 280:468–473.

Beth, A. H., K. Balasubramanian, B. H. Robinson, L. R. Dalton, S. D. Venkataramu, and J. H. Park. 1983. Sensitivity of V_2' saturation transfer electron paramagnetic resonance signals to anisotropic rotational diffusion with [^{15}N]nitroxide spin-labels: effects of noncoincident magnetic and diffusion tensor principal axes. *J. Phys. Chem.* 87:359–367.

Beth, A. H., K. Balasubramanian, R. T. Wilder, S. D. Venkataramu, B. H. Robinson, L. R. Dalton, D. E. Pearson, C. R. Park, and J. H. Park. 1981. Structural and motional changes in glyceraldehyde-3-phosphate dehydrogenase upon binding to band 3 protein of the red blood cell membrane examined with [^{15}N,^{2}H] maleimide spin label and EPR. *Proc. Natl. Acad. Sci. U.S.A.* 78:4955–4959.

Beth, A. H., and B. H. Robinson. 1989. Nitrogen-15 and deuterium substituted spin labels for studies of very slow rotational motion. *In* Biological Magnetic Resonance, Vol. 8: Spin Labeling: Theory and Applications. L. J. Berliner and J. Reuben, editors. Plenum Press, New York.179–253.

Blackman, S. M., C. E. Cobb, A. H. Beth, and D. W. Piston. 1996. The orientation of eosin-5-maleimide on human erythrocyte band 3 measured by fluorescence polarization microscopy. *Biophys. J.* 71:194–208.

Blackman, S. M., E. J. Hustedt, C. E. Cobb, and A. H. Beth. 1999. Flexibility of the link between the cytoplasmic and membrane spanning domains of erythrocyte band 3. *Biophys. J.* 76:A233.

Blackman, S. M., D. W. Piston, and A. H. Beth. 1998a. Oligomeric state of human erythrocyte band 3 measured by fluorescence resonance energy homotransfer. *Biophys. J.* 75:1117–1130.

Blackman, S. M., D. W. Piston, and A. H. Beth. 1998b. Self-association of human erythrocyte band 3 in situ: a simple fluorescence assay based on resonance energy homotransfer. *Biophys. J.* 74:A393.

Casey, J. R., and R. A. F. Reithmeier. 1991. Analysis of the oligomeric state of band 3, the anion transport protein of the human erythrocyte membrane, by size exclusion high performance liquid chromatography. *J. Biol. Chem.* 266:15726–15737.

Cassoly, R. 1982. Interaction of hemoglobin with the red blood cell membrane: a saturation transfer electron paramagnetic resonance study. *Biochim. Biophys. Acta.* 689:203–209.

Che, A., and R. J. Cherry. 1995. Loss of rotational mobility of band 3 proteins in human erythrocyte membranes induced by antibodies to glycophorin A. *Biophys. J.* 68:1881–1887.

Cobb, C. E., and A. H. Beth. 1990. Identification of the eosinyl-5-maleimide reaction site on the human erythrocyte anion exchange protein: overlap with the reaction sites of other chemical probes. *Biochemistry.* 29:8283–8290.

Cobb, C. E., E. J. Hustedt, J. M. Beechem, and A. H. Beth. 1993. Protein rotational dynamics investigated with a dual EPR/optical molecular probe: spin-labeled eosin. *Biophys. J.* 64:605–613.

Corbett, J. D., and D. E. Golan. 1993. Band 3 and glycophorin are progressively aggregated in density-fractionated sickle and normal red blood cells. *J. Clin. Invest.* 91:208–217.

Fairbanks, G., T. L. Steck, and D. F. H. Wallach. 1971. Electrophoretic analysis of the major polypeptides of the human erythrocyte membrane. *Biochemistry.* 10:2606–2617.

Golan, D. E., J. D. Corbett, C. Korsgren, H. S. Thatte, S. Hayette, Y. Yawata, and C. M. Cohen. 1996. Control of band 3 lateral and rotational mobility by band 4.2 in intact erythrocytes: release of band 3 oligomers from low-affinity binding sites. *Biophys. J.* 70:1534–1542.

Hall, T. G., and V. Bennett. 1987. Regulatory domains of erythrocyte ankyrin. *J. Biol. Chem.* 262:10537–10545.

Hustedt, E. J., and A. H. Beth. 1995. Analysis of saturation-transfer electron paramagnetic resonance spectra of a spin-labeled integral membrane protein, band 3, in terms of the uniaxial rotational diffusion model. *Biophys. J.* 69:1409–1423.

Hustedt, E. J., and A. H. Beth. 1996. Determination of the orientation of a band 3 affinity spin-label relative to the membrane normal axis of the human erythrocyte. *Biochemistry.* 35:6944–6954.

Hustedt, E. J., and A. H. Beth. 2001. *Biophys. J.* In press.

Hustedt, E. J., S. M. Blackman, C. E. Cobb, and A. H. Beth. 2000. Effects of constrained uniaxial rotational diffusion on ST-EPR spectra: application to band 3 in human erythrocytes. *Biophys. J.* 78:382A.

Hustedt, E. J., C. E. Cobb, A. H. Beth, and J. M. Beechem. 1993. Measurement of rotational dynamics by the simultaneous non-linear analysis of optical and EPR data. *Biophys. J.* 64:614–621.

Jarolim, P., J. Palek, D. Amoto, K. Hassan, P. Sapak, G. T. Nurse, H. L. Rubin, S. Zhai, K. E. Sahr, and S.-C. Liu. 1990. Deletion in erythrocyte band 3 gene in malaria-resistant Southeast Asian ovalocytosis. *Proc. Natl. Acad. Sci. U.S.A.* 88:11022–11026.

Knauf, P. A. 1979. Erythrocyte anion exchange and the band 3 protein: transport kinetics and molecular structure. *Curr. Top. Membr. Transp.* 12:249–363.

Laemmli, U. K. 1970. Cleavage of structural proteins during the assembly of the head of bacteriophage T4. *Nature.* 227:680–685.

Lepke, S., and H. Passow. 1976. Effects of incorporated trypsin on anion exchange and membrane proteins in human red blood cell ghosts. *Biochim. Biophys. Acta.* 455:353–370.

Low, P. S. 1986. Structure and function of the cytoplasmic domain of band 3: center of erythrocyte membrane-peripheral protein interactions. *Biochim. Biophys. Acta.* 864:145–167.

Low, P. S., M. A. Westfall, D. P. Allen, and K. C. Appell. 1984. Characterization of the reversible conformational equilibrium of the cytoplasmic domain of erythrocyte membrane band 3. *J. Biol. Chem.* 259: 13070–13076.

Lux, S. E., K. M. John, R. R. Kopito, and H. F. Lodish. 1989. Cloning and characterization of band 3, the human erythrocyte anion-exchange protein (AE1). *Proc. Natl. Acad. Sci. U.S.A.* 86:9089–9093.

Lux, S. E., and J. Palek. 1995. Disorders of the red cell membrane. *In* Blood: Principles and Practice of Hematology. R. I. Handin, S. E. Lux, and T. P. Stossel, editors. Lippincott, Philadelphia. 1701–1718.

Matayoshi, E. D., and T. M. Jovin. 1991. Rotational diffusion of band 3 in erythrocyte membranes. I. Comparison of ghosts and intact cells. *Biochemistry.* 30:3527–3538.

McPherson, R. A., W. H. Sawyer, and L. Tilley. 1992. Rotational diffusion of the erythrocyte integral membrane protein band 3: effect of hemichrome binding. *Biochemistry.* 31:512–518.

McPherson, R. A., W. H. Sawyer, and L. Tilley. 1993. Band 3 mobility in camelid elliptocytes: implications for erythrocyte shape. *Biochemistry.* 32:6696–6702.

Michaely, P., and V. Bennett. 1995. The ANK repeats of erythrocyte ankyrin form two distinct but cooperative binding sites for the erythrocyte anion exchanger. *J. Biol. Chem.* 270:22050–22057.

Moriyama, R., H. Ideguchi, C. R. Lombardo, H. M. Van Dort, and P. S. Low. 1992. Structural and functional characterization of band 3 from Southeast Asian ovalocytes. *J. Biol. Chem.* 267:25792–25797.

Nigg, E. A., and R. J. Cherry. 1980. Anchorage of a band 3 population at the erythrocyte cytoplasmic membrane surface: protein rotational diffusion measurements. *Proc. Natl. Acad. Sci. U.S.A.* 77:4702–4706.

Oikawa, K., D. M. Lieberman, and R. A. F. Reithmeier. 1985. Conformation and stability of the anion transport protein of human erythrocyte membranes. *Biochemistry.* 24:2843–2848.

Peters, L. L., R. A. Shivdasani, S.-C. Liu, M. Hanspal, K. M. John, J. M. Gonzalez, C. Brugnara, B. Gwynn, N. Mohandas, S. L. Alper, S. H. Okrin, and S. E. Lux. 1996. Anion exchanger 1 (band 3) is required to prevent erythrocyte membrane surface loss but not to form the membrane skeleton. *Cell.* 86:917–927.

Rybicki, A. C., R. S. Schwartz, E. J. Hustedt, and C. E. Cobb. 1996. Increased rotational mobility and extractability of band 3 from protein

4.2-deficient erythrocyte membranes: evidence of a role for protein 4.2 in strengthening the band 3-cytoskeleton linkage. *Blood.* 88:2745–2753.

Schofield, A. E., M. J. A. Tanner, J. C. Pinder, B. Clough, P. M. Bayley, G. B. Nash, A. R. Dluzewski, D. M. Reardon, T. M. Cox, R. J. Wilson, and W. B. Gratzer. 1992. Basis of unique red cell membrane properties in hereditary ovalocytosis. *J. Mol. Biol.* 223:949–958.

Scothorn, D. J., W. E. Wojcicki, E. J. Hustedt, A. H. Beth, and C. E. Cobb. 1996. Synthesis and characterization of a novel spin-labeled affinity probe of human erythrocyte band 3: characterization of the stilbenedisulfonate binding site. *Biophys. J.* 35:6931–6943.

Southgate, C. D., A. H. Chishti, B. Mitchell, S. J. Yi, and J. Palek. 1996. Targeted disruption of the murine erythroid band 3 gene results in spherocytosis and severe haemolytic anaemia despite a normal membrane skeleton. *Nat. Genet.* 14:227–230.

Steck, T. L., B. Ramos, and E. Strapazon. 1976. Proteolytic dissection of band 3, the predominant transmembrane polypeptide of the human erythrocyte membrane. *Biochemistry.* 15:1153–1161.

Szabo, A. 1984. Theory of fluorescence depolarization in macromolecules and membranes. *J. Chem. Phys.* 81:150–167.

Tanner, M. J. 1997. The structure and function of band 3 (AE1): recent developments. *Mol. Membr. Biol.* 14:155–165.

Tanner, M. J., P. G. Martin, and S. High. 1988. The complete amino acid sequence of the human erythrocyte membrane anion-transport protein deduced from the cDNA sequence. *Biochem. J.* 256:703–712.

Thevenin, B. J.-M., and P. S. Low. 1990. Kinetics and regulation of the ankyrin-band 3 interaction of the human red blood cell membrane. *J. Biol. Chem.* 265:16166–16172.

Thomas, D. D., L. R. Dalton, and J. S. Hyde. 1976. Rotational diffusion studied by passage saturation transfer electron paramagnetic resonance. *J. Chem. Phys.* 65:3006–3024.

Turrini, F., A. Paolo, J. Yuan, and P. S. Low. 1991. Clustering of integral membrane protein of the human erythrocyte membrane stimulates autologous IgG binding, complement deposition, and phagocytosis. *J. Biol. Chem.* 266:23611–23617.

Wahl, Ph. 1975. Fluorescence anisotropy of chromophores rotating between two reflecting barriers. *Chem. Phys.* 7:210–219.

Wang, D. N., W. Kuhlbrandt, V. E. Sabina, and R. A. F. Reithmeier. 1993. Two dimensional structure of the membrane domain of human band 3, the anion transport protein of the erythrocyte membrane. *EMBO J.* 12:2233–2239.

Wang, D. N. 1994. Band 3 protein: structure, flexibility, and function. *FEBS Lett.* 346:26–31.

Weinstein, R. S., J. K. Khodadad, and T. L. Steck. 1978. Fine structure of the band 3 protein in human red cell membranes: freeze-fracture studies. *J. Supramol. Struct.* 8:325–335.

Willardson, B. M., B. J.-M. Thevenin, M. L. Harrison, W. M. Kuster, M. D. Benson, and P. S. Low. 1989. Localization of the ankyrin-binding site on erythrocyte membrane protein, band 3. *J. Biol. Chem.* 264: 15893–15899.

Yi, S. J., S.-C. Liu, L. H. Derick, J. Murray, J. E. Barker, M. R. Cho, J. Palek, and D. E. Golan. 1997. Red blood cell membranes of ankyrin-deficient nb/nb mice lack band 3 tetramers but contain normal membrane skeletons. *Biochemistry.* 36:9596–9604.

Zhang, D., A. Kiyatkin, J. T. Bolin, and P. S. Low. 2000. Crystallographic structure and functional interpretation of the cytoplasmic domain of erythrocyte membrane band 3. *Blood.* 96:2925–2933.